Int. J. Electrochem. Sci., 17 **(2022)** Article Number: 220241, doi: 10.20964/2022.02.08

International Journal of
ELECTROCHEMICAL
SCIENCE
www.electrochemsci.org

Preparation of Platinum Decorated Laser-Induced Graphene Flexible Electrode and Its Application for Clenbuterol Detection

Hongwei Tang[1,!], *Ying Zhong*[2,5,!], *Xiangrong Zeng*[2,5,!], *Yu Sang*[2,3], *Furui Lin*[2], *Yifu Zhu*[2], *Zhongping Chen*[4,*], *Lanjiao Xu*[3], *Zhong Huang*[2], *Peicong Zhou*[5,*]

[1] College of Computer and Information Engineering, Jiangxi Agricultural University, Nanchang 330045, China
[2] College of Chemistry and Materials, Jiangxi Agricultural University, Nanchang 330045, China
[3] Jiangxi Province Key Laboratory of Animal Nutrition/Engineering Research Center of Feed Development, Jiangxi Agricultural University, Nanchang 330045, China
[4] Agricultural Technology Extension Center of Jiangxi Province, Nanchang 330046, China
[5] College of Engineering, Jiangxi Agricultural University, Nanchang 330045, China
[*]E-mail: czpjxaas@163.com, pc.zhou@jxau.edu.cn

Received: 27 October 2021 / *Accepted:* 29 November 2021 / *Published:* 5 January 2022

The traditional preparation method of graphene is complicated in operation and high-cost, which severely limits the further application of graphene. Hence, a new strategy for the rapid, large-scale, low-cost preparation of graphene can effectively solve the current problems. In this work, laser-induced graphene (LIG) was rapidly prepared in one step based on polyimide (PI) film as the substrate, by using laser direct writing technology, and prepare LIG into a flexible electrode. Besides that, LIG flexible electrode was modified the by chemical method, sodium borohydride was used as reducing agent to reduce chloroplatinic acid, and Pt metal nanoparticles were loaded on the surface of LIG electrode in situ to prepare Pt-LIG composite electrode material. Compared with LIG electrode, Pt-LIG electrode has high conductivity, larger surface area and better electrocatalytic ability. It is used as a new type of electrochemical sensing platform to perform electrochemical detection of clenbuterol (CLB), obtaining a wide detection linear range of 0.1 – 820.9 μM, and a lower limit of detection (LOD) of 0.072 μM. Moreover, the CLB in the actual sample of beef was detected at the same time, and an effective and acceptable recovery rate was obtained.

Keywords: Laser-induced graphene; Pt nanoparticles; Flexible electrode; Electrochemical sensor; Clenbuterol.

1. INTRODUCTION

In recent years, nanomaterials have received extensive attention from researchers, especially carbon-based materials, which exhibit excellent electrical conductivity, large specific surface area and good biocompatibility, and have active applications in biosensors, energy storage devices, etc [1, 2]. Graphene has become a widely used material in the field of electrochemical analysis due to its excellent electronic transfer rate, large specific surface area and other excellent physical and chemical properties [3-5]. So far, researchers have developed a variety of graphene preparation methods, including mechanical peeling method [6], sometimes referred to as scotch tape method, thermal decomposition method [7], chemical vapor deposition method [8], and thermal reduction oxidation method [9, 10]. In 2014, Tour's group [11] first proposed a new method for fast and easy preparation of graphene. By direct laser irradiation of polyimide (PI) film, flexible commercial PI film can be converted into graphene. This preparation of resulting material is called laser-induced graphene (LIG) [12, 13]. During laser irradiation, the sp^3 carbon atoms in the polyimide are converted into sp^2 carbon atoms by photothermal catalysis, which has better conductivity [3, 14]. The C-O, C=O and C≡N in the polyimide will be broken, recombined and released in the form of gas, resulting in a honeycomb-like porous graphene nanosheet with a hexagonal lattice structure [11, 15]. Its structure contains a large amount of carbon and a small amount of oxygen, which makes LIG have a larger surface area. In addition, LIG also has other advantages, including simple and fast preparation, no need for high-temperature reaction conditions, solvents or subsequent treatments like conventional synthetic methods, high chemical stability and low cost, all of which make it have wide range of practicality [16, 17].

Metal nanoparticles are also a kind of nanomaterials. Nanoparticles are small in size, large in surface area, and have high electrochemical catalytic activity [18]. Platinum nanoparticles may be considered as the most effective catalytic material due to their excellent electrical conductivity and electrocatalytic activity [19, 20]. The usual method for preparing metal nanoparticles is to reduce metal ions by chemical or electrochemical methods. In order to prevent the agglomeration of the generated nanoparticles, a certain amount of protective agent is generally added during the reduction process to stabilize the generated particles [21].

Clenbuterol hydrochloride (CLB) [22] is an adrenal nerve stimulant, which has a high selective agonizing effect on bronchial smooth muscle [23, 24]. In clinical medicine, it can be used to prevent and treat bronchial asthma, wheezing bronchospasm and other respiratory diseases [25]. At the same time, CLB can also promote the conversion and decomposition of fatty acids and the synthesis of protein. For this reason, it is often illegally added to animal feed or veterinary drugs by illegal businesses to increase the lean meat ratio of animals [26]. Therefore, CLB is also called "Clenbuterol". After being eaten by animals, CLB can form accumulated residues in the internal organs, and cause harm to human health through the food chain and cause symptoms of poisoning.

Therefore, in order to ensure food safety, it is necessary to develop a fast, simple, and sensitive detection method to analyze the CLB residues in meat products. Combined with previous work [27-29], a laser-induced graphene (LIG) flexible electrode was designed as a substrate, sodium borohydride was used as a reducing agent through a chemical method to reduce chloroplatinic acid, and metal nanoparticles Pt were in-situ loaded on the surface of the LIG electrode. The prepared Pt-LIG composite

electrode is constructed as an electrochemical sensor, which realizes the sensitive and rapid detection of CLB.

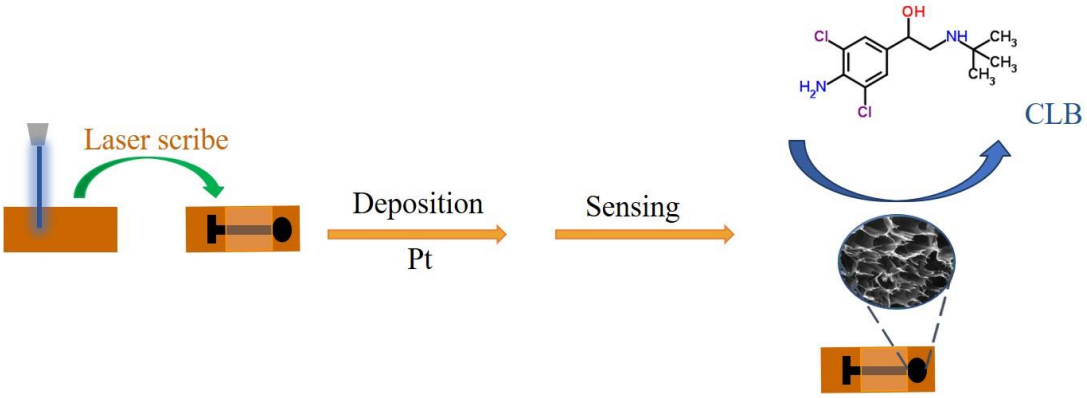

Figure 1. Preparation of Pt-LIG composite electrode and its sensing application to CLB.

2. EXPERIMENTAL

2.1 Materials and apparatus

Polyimide film was purchased from DuPont Company, America (thickness: 75 μm). Clenbuterol, sodium borohydride, chloroplatinic acid and other reagents were obtained from Shanghai Aladdin Biochem. Tech. Co. Ltd., China. 0.1 M Britton-Robinson (B-R) Buffer Solution were used prepared by 0.04 M H_3PO_4, HAc and H_3BO_3. Deionized water (DI water) was obtained from a Milli-Q water purification system.

Scanning electron microscopy (SEM, FEI Company, QUANTA Q400, United States) and energy-dispersive X-ray spectroscopy (EDS, EDAX Company, United States) were employed to observe morphology and elemental composition characteristics of LIG electrode.

2.2 Preparation of LIG electrode

PI film as the substrate, the surface of PI film was cleaned with absolute ethanol and deionized water, and then dried. The PI film was fixed and designed a specific electrode shape through computer patterning, including a circle area with a diameter of 3 mm was used as the effective working area, and finally the laser-induced graphene (LIG) electrode could be prepared by emitting a pulsed laser on the surface of the PI film through a laser direct writer [16].

2.3 Preparation of Pt-LIG modified electrode

Sodium borohydride as a reducing agent was added into 5 μM chloroplatinic acid solution, subsequently immersed the effective working area of the prepared LIG electrode in the solution, magnetic stirring at room temperature for 4 hours. and then the electrode was dried in an oven at 60 °C

for 2 hours, so that the Pt nanoparticles were reduced on the surface of the LIG electrode, finally, the Pt-LIG electrode was prepared.

2.4 Electrochemical detection

5 mL of 0.1 M B-R solution (pH = 3.0) were added into the electrolytic cell with a pipette as the electrolyte solution, then a certain concentration of clenbuterol CLB was added into the electrolyte solution, and CLB was detected by differential pulse voltammetry (DPV). All Electrochemical measurements were performed using CHI 660E electrochemical workstation, the three-electrode system was composed of LIG electrode, platinum wire (Pt) and saturated calomel electrode (SCE). All measurements were carried out in surrounding environment.

2.5 Real sample preparation

The beef sample was obtained from the College of Animal Science, Jiangxi Agricultural University. The beef sample was treated with ethyl acetate, after shaking for 20 minutes, it was centrifuged at room temperature (11000 rpm, 15 min), the supernatant was taken, and then ethyl acetate was used for precipitation treatment, the supernatant obtained was the real sample required. Then a certain amount of real sample solution was diluted in 0.1 M B-R (pH = 3.0), and detected the content of CLB by DPV in the real sample under optimal conditions.

3. RESULTS AND DISCUSSION

3.1 Morphology of LIG and Pt-LIG electrodes

The morphologies of LIG and Pt-LIG were characterized by SEM-EDS. As can be seen in the SEM images (Figure 2A-C), the prepared LIG surface presents an obvious 3D porous structure. The C-O, C=O and C≡N in the polyimide will be broken, recombined and released quickly in the form of gaseous products [15], resulting in a honeycomb-like hexagonal lattice structure. Corresponding to the EDS image (Figure 3), it shows that LIG only contains a large amount of C element and a small amount of O element, while the raw material polyimide contains N element, which indicates that the gaseous product produced were likely to be nitrogen oxides during the laser action. These porous structures formed on the LIG surface greatly increase the effective surface area and conduce to the electrolyte to penetrate into the active material. In the SEM images (Figure 2D-F), it can be seen that some spherical nanoparticles are attached to the porous structure of the prepared Pt-LIG surface. In the corresponding EDS image (Figure 3), in addition to the large amount of C element and a small amount of O element originally contained in LIG, a small amount of Pt element is also added, suggesting that these nanoparticles are Pt nanoparticles, and Pt-LIG materials have also been successfully prepared. In addition, nanoparticles with a spherical structure also provide a larger surface area for contact sites.

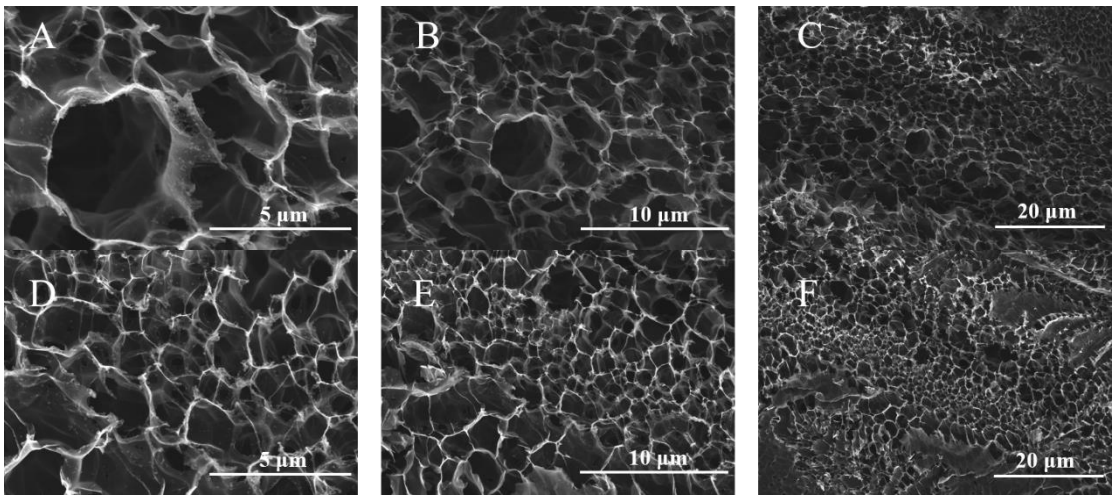

Figure 2. SEM images of LIG (A-C) and Pt-LIG (D-F) electrode.

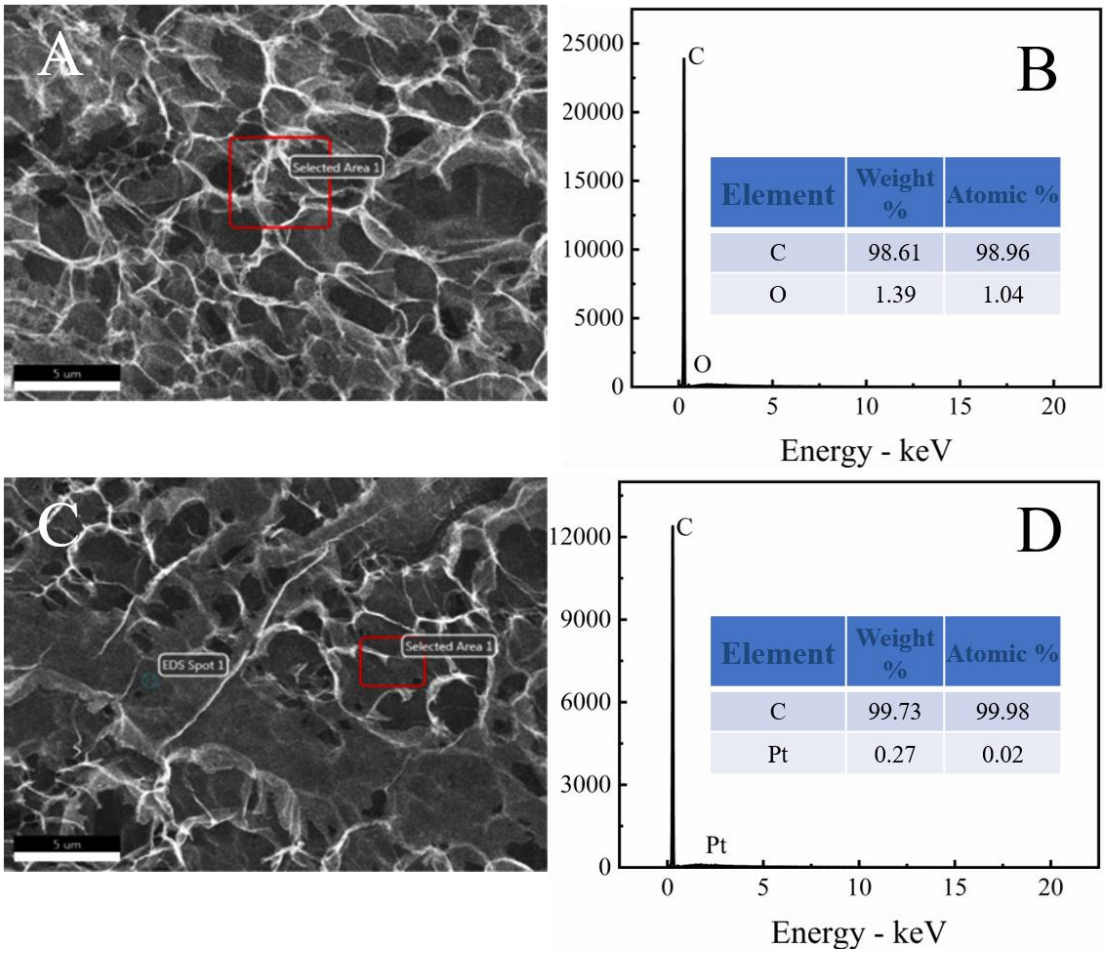

Figure 3. EDS analysis of LIG (A-B) and Pt-LIG (C-D) electrode.

3.2 Electrochemical performance of LIG and Pt-LIG electrodes

The LIG and Pt-LIG electrodes were tested for electrochemical impedance in 5 mM $[Fe(CN)_6]^{3-/4}$ solution containing 0.1 M KCl, respectively. The Nyquist chart of electrochemical impedance spectroscopy (EIS) contains a semicircular part and a linear part. The higher frequency of the semicircular part represents the process of limited electron transfer. The diameter of the semicircle can be used to evaluate the electron transfer resistance (R_{ct}), while the lower frequency of the linear part represents the diffusion process. [35]. As shown in Figure 4, LIG has a semicircular part, and the diameter of the semicircle is small, indicating that the prepared LIG electrode as a carbon nanomaterial has good electron transfer ability and excellent conductivity. While Pt nanoparticles are modified on the surface of the LIG electrode, it can be found that the diameter of the semicircle of Pt-LIG decreases by about half in Nyquist plot. Which shows that Pt nanoparticles contribute to the improvement of electron transfer ability. Suggesting that Pt-LIG has better conductivity than LIG. However, the higher frequency and lower frequency tend to be a straight line, it shows that the reaction of electrode is controlled by diffusion process.

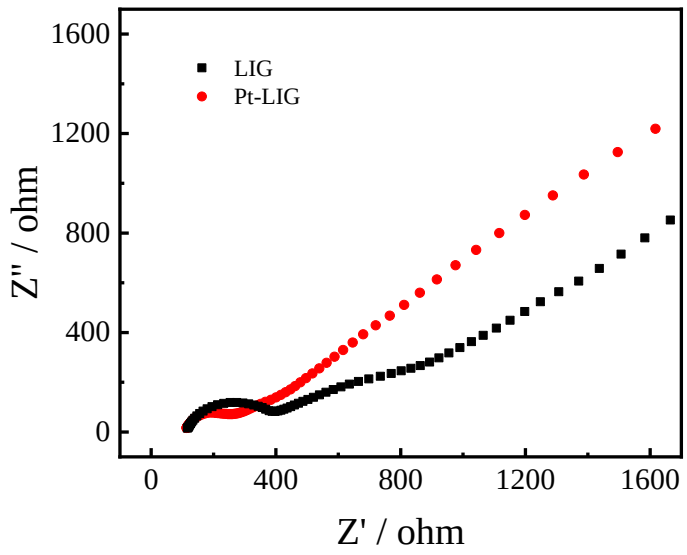

Figure 4. Nyquist plots of LIG and Pt-LIG electrodes in 5 mM $[Fe(CN)_6]^{3-/4-}$ containing 0.1 M KCl.

In order to further study the electrochemical performance of LIG and Pt-LIG electrodes, which were scanned at different scan rates (50, 100, 150, 200, 250, 300, 350, 400, 450 and 500 mV/s) by cyclic voltammetry in 5 mM $[Fe(CN)_6]^{3-}$ solution containing 0.1 M KCl, to study the electrochemical effective area of different electrodes. According to the Randles-Sevick equation:

$$I_{p,a} = 2.69 \times 10^5 n^{3/2} A C_0 D_R^{1/2} v^{1/2}$$

Where $I_{p,a}$ is the peak oxidation current, n is the number of electrons transferred, A is the effective surface area, C_0 is the concentration of $[Fe(CN)_6]^{3-}$, D_R is the diffusion coefficient, v is the scan rate, n = 1, $D_R = 7.6 \times 10^{-6}$ cm s^{-1}. According to the slope of the equation of linear fitting between oxidation

peak current ($I_{p,a}$) and scan rate to the 1/2 power ($v^{1/2}$) of LIG and Pt-LIG electrodes in $[Fe(CN)_6]^{3-}$ solution in Figure 5. The electrochemically active areas of LIG and Pt-LIG electrodes can be calculated as 0.0087 cm^2 and 0.015 cm^2, respectively. It can be seen that the electrochemically active area of the modified electrode Pt-LIG is nearly twice that of LIG, which greatly improves the electron transfer rate.

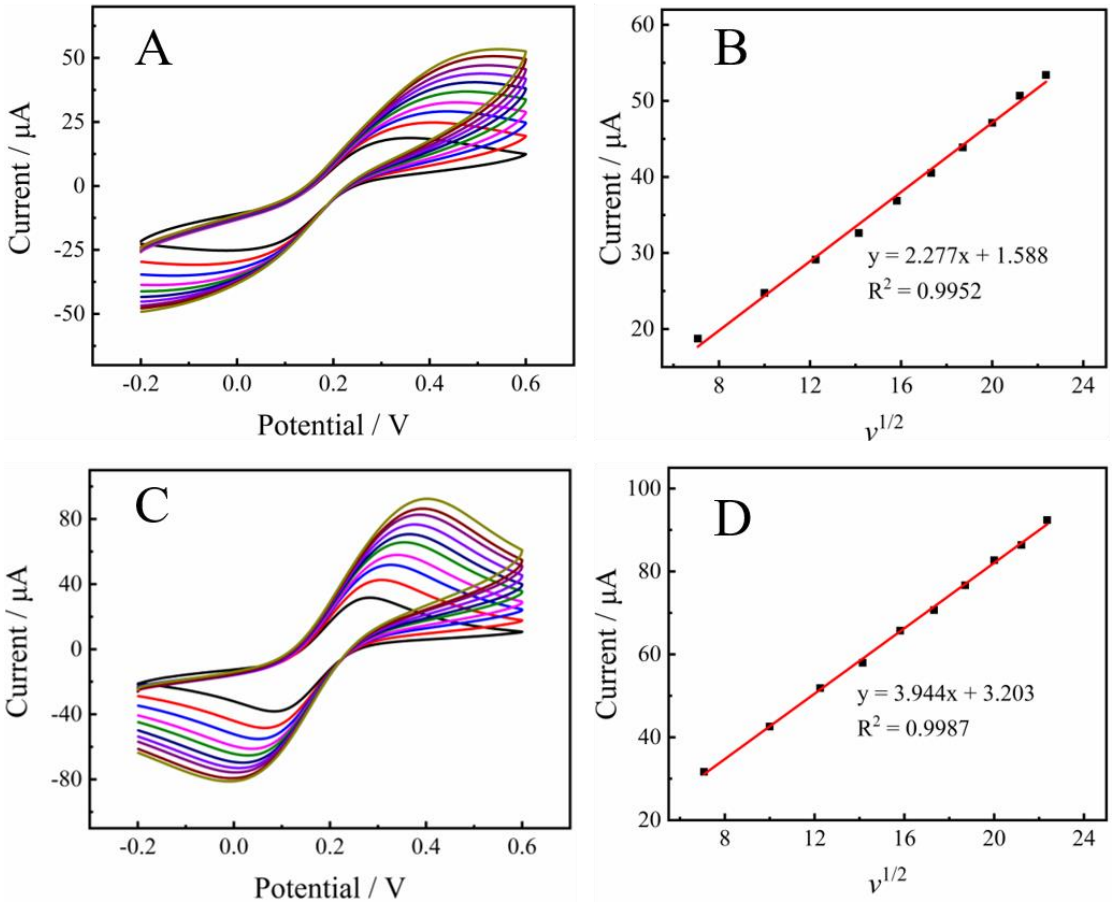

Figure 5. Cyclic voltammograms and corresponding oxidation peak currents and square root scan rates of LIG and Pt-LIG electrodes in 5 mM $[Fe(CN)_6]^{3-}$ containing 0.1 M KCl.

3.3 Electrochemical behavior of LIG and Pt-LIG electrodes

As shown in the Figure 6, 20 μM CLB were detected by the LIG and Pt-LIG electrodes through DPV in 0.1 M B-R buffer (pH = 3.0). Including that, a weak and asymmetric oxidation peak was seen on LIG. While Pt nanoparticles were modified, due to Pt nanoparticles has excellent conductivity and good electrocatalytic activity on CLB, a larger response current and a more symmetrical oxidation peak was seen on Pt- LIG, which also demonstrated that the Pt-LIG composite has stronger electrocatalytic performance for CLB and has a faster electron transfer rate. Suggesting that Pt nanoparticles increasing the specific surface area of LIG and has a synergistic effect of high electrocatalytic activity, which makes

Pt-LIG has a better electrochemical response to CLB. Therefore, Pt-LIG can be well applied to the electrochemical detection of CLB.

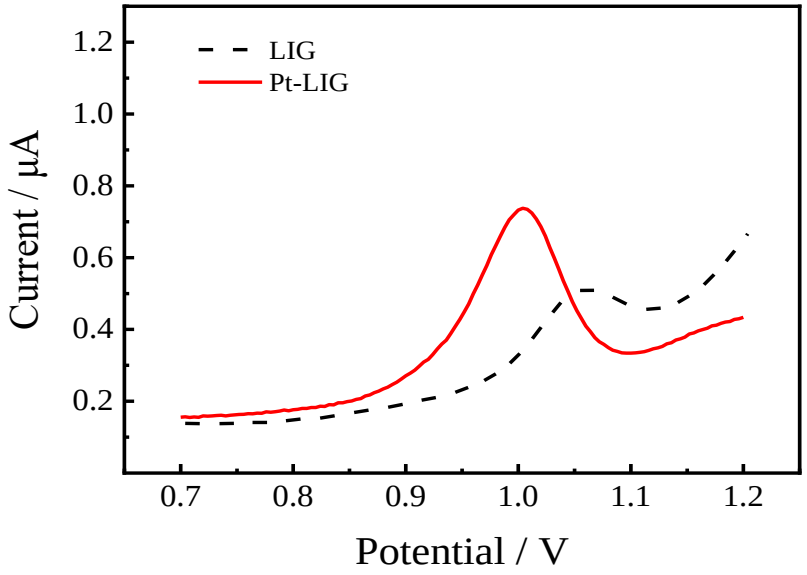

Figure 6. DPV of at LIG and Pt-LIG electrodes in 0.1 M B-R (pH = 3.0) contain 20 μM CLB.

3.4 Parametric optimization of Pt-LIG electrode

Figure 7 (A) shows 20 μM CLB were detected by CV on the modified electrode Pt-LIG at different scanning rates (50, 100, 150, 200, 250, 300, 350, 400, 450 and 500 mV s^{-1}) in 0.1 M B-R (pH = 3.0). As shown in Figure 7 (B), as the scan rate (v) increases, the oxidation peak current ($I_{p,a}$) also gradually increases, and $I_{p,a}$ has a linear relationship with the v by linear fitting:

$I_{p,a} = 0.005v + 0.385$ $R^2 = 0.9951$

It shows that Pt-LIG is a typical adsorption control process for electrochemical detection of CLB. According to Laviron theory and Langmuir isotherm adsorption equation [36]:

$$I_p = n^2F^2vA\Gamma_T / 4RT = nFQv / 4RT$$

Where I_p is the anode peak current, n is the number of electron transfers, A is the effective surface area, v is the scan rate, Γ_T is the surface coverage concentration, Q is the amount of electricity, R = 8.314 J mol^{-1} K^{-1}, T = 298 K, F = 96485 C mol^{-1}. Therefore:

take v_1 = 0.1 V s^{-1} and v_2 = 0.15 V s^{-1} as examples,

$I_{p,1} = 8.85\times10^{-7}$ A， $Q_1 = 4.475\times10^{-7}$ C；

$I_{p,2} = 11.35\times10^{-7}$ A， $Q_2 = 3.624\times10^{-7}$ C；

It can be calculated that the number of electrons involved in the reaction is 2.03 and 2.14 respectively, which can be approximately 2.

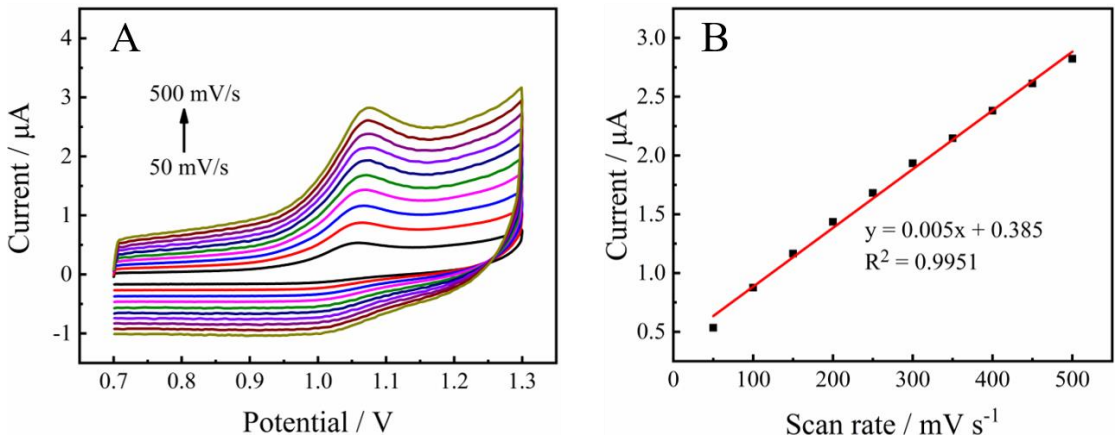

Figure 7. (A) CVs of Pt-LIG electrodes in 0.1 M B-R (pH = 3.0) contain 20 μM CLB with different scan rates: 100, 150, 200, 250, 300, 350, 400, 450 and 500 mV s^{-1}; the linear relationship of $I_{p,a}$ and *v*.

In order to study the influence of the pH value of the electrolyte solution on the peak current ($I_{p,a}$) and peak potential ($E_{p,a}$), CLB was detected at Pt-LIG electrode by DPV in a 0.1 M B-R with a pH range of 2.0 to 6.0. As shown in Figure 8 (A), as the pH value increases from 2.0 to 6.0, the peak current $I_{p,a}$ of the CLB first increases and then gradually decreases. The maximum current value is reached when pH = 3.0, suggesting that pH = 3.0 is the best pH value for electrochemical detection.

In addition, as shown in Figure 8(B), the peak potential ($E_{p,a}$)of the CLB decreases with the increase of pH, that is shifts to the negative direction, which indicates that protons directly participate in the oxidation reaction of CLB, and $E_{p,a}$ has a linear relationship with pH. The relationship between $E_{p,a}$ and pH can be expressed as:

$E_{p,a}$ = -0.054 pH + 1.16（R^2 = 0.9723）

It can be seen that the slope of the equation -0.054 V pH^{-1} is close to the theoretical value of -0.059 V pH^{-1}, which indicates that the Pt-LIG electrode involves the same number of electrons and protons in the electrochemical oxidation process. According to the scanning rate section 3.4, the electron transfer number (n) has been calculated to be 2, therefore it can be inferred that the oxidation process of CLB on Pt-LIG involves two electrons and two protons in the reaction.

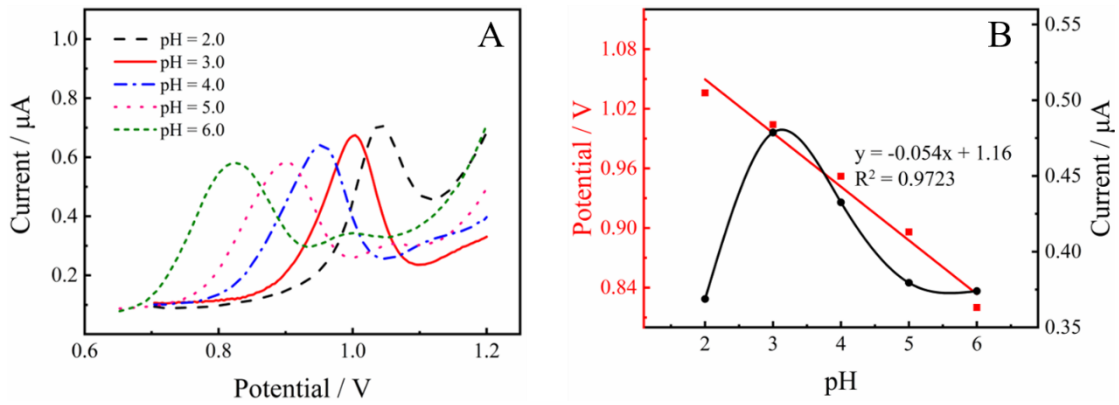

Figure 8. (A) DPV of CLB at Pt-LIG with different pH values, (B) Effect of pH on the peak current and the peak potentials.

3.5 Electrochemical detection of CLB

Different concentrations of CLB were detected by DPV at Pt-LIG electrodes in optimal conditions. As shown in Figure 9, the oxidation peak current ($I_{p,a}$) increases with the increase of the CLB concentrations range from 0.1-820.9 μM, and the increment becomes smaller and tends to gentle. It is found that the oxidation peak current ($I_{p,a}$) is proportional to analyte concentrations to the 1/2 power ($C^{1/2}$) by linear fitting. The linear fitting equation is:

$I_{p,a} = 0.2383C - 0.1879$ ($R^2 = 0.9925$)

The limit of detection (LOD) of CLB (S/N = 3) can be estimated to be 0.072 μM, and the LOQ is 0.24 μM. And the sensitivity is estimated by the slope of the calibration curve, so the sensitivity for CLB is 0.2383 μA μM^{-1}.

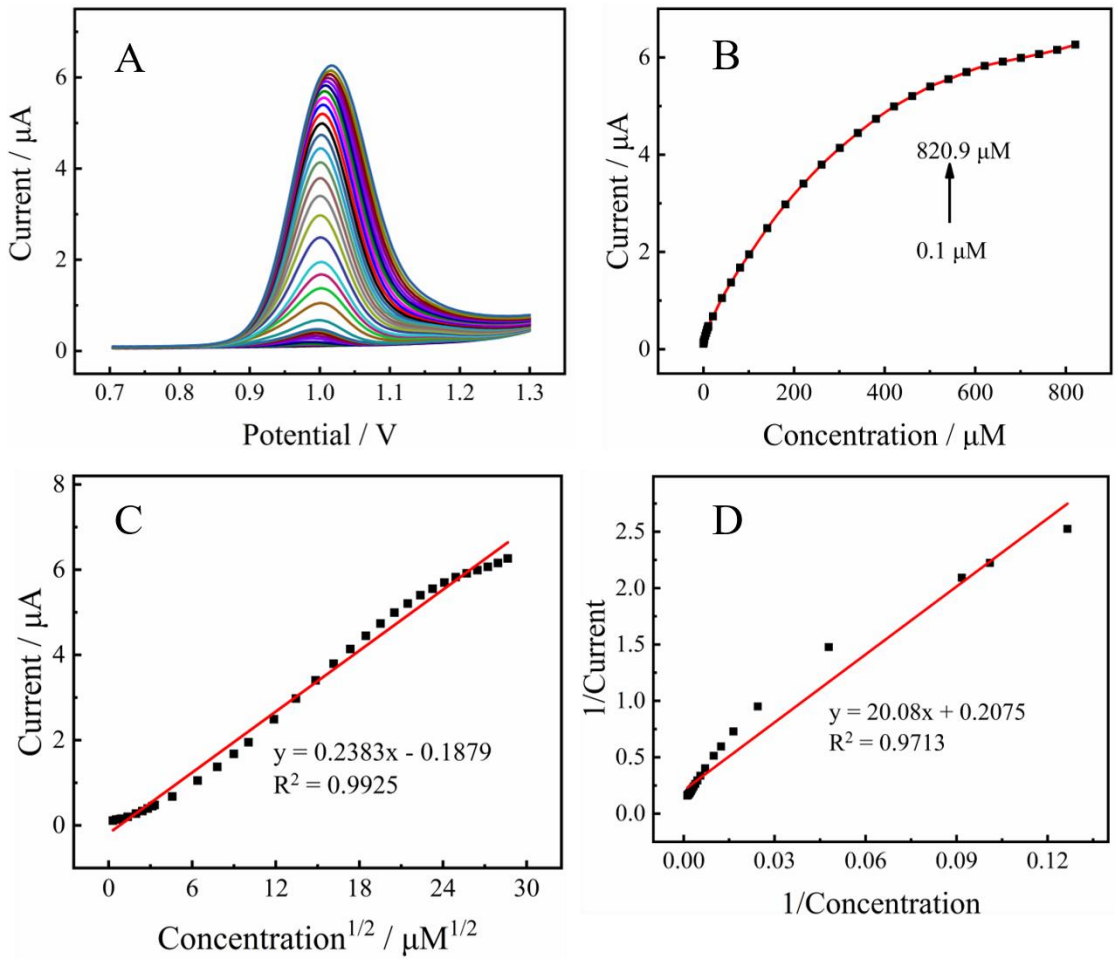

Figure 9. (A) DPV of CLB with different concentrations on Pt-LIG; (B)The relationship of $I_{p,a}$ and concentrations of CLB; (C) The relationship of $I_{p,a}$ and $C^{1/2}$; (D) The relationship between the inverse of $I_{p,a}$ and the inverse of concentration.

At the same time, it is found that the reciprocal of $I_{p,a}$ ($1/I_{p,a}$) is also proportional to the reciprocal of concentration ($1/C$) by linear fitting, the equation as follows:

$1/I_{p,a} = 20.08/C + 0.2075$ ($R^2 = 0.9713$)

Corresponds to the previous work [37, 38], the inverse of the oxidation peak current is proportional to the inverse of the analyte concentration. It can be inferred that Pt-LIG also has enzyme-like properties. According to the Michaelis-Menten equation, it can be calculated that K_m = 96.77 μM, I_{max} = 4.82 μA.

Furthermore, the recent studies [26, 30-34] on the electrochemical sensor for clenbuterol determination are shown in the Table 1.

Table 1. The comparison of the sensor with similar sensors for clenbuterol determination

Modified electrodes	Methods	Analytes	Linear ranges (μM)	LOD (μM)	Applications	Reference
IP-Nf (BP)/GCE	DPV	CLB	0.06 - 24	0.0037	Bovine meat and bovine serum	[26]
OMC/GCE	DPV	CLB	0.085 - 8.0	0.06	Pork	[30]
Isopropanol–Nafion–PSS–GR/GCE	LSV	CLB	0.075 - 25	0.022	Pork	[31]
MIP-CNSQ/WGE	CV	CLB	0.3 - 50	0.01	Pork	[32]
Graphene oxide/GCE	DPV	CLB	0.0797 - 3.19	0.0478	Pork	[33]
S-β-CD-BP-PEDOTs	DPV	CLB RAC	0.3 - 90 0.3 - 9.4	0.12 0.14	Beef Feed Bovine serum	[34]
Pt-LSG	DPV	CLB	0.1 - 820.9	0.072	Beef	This work

3.6 Real samples

In order to study the practicability of Pt-LIG, the CLB was detected in beef samples by the standard addition method. The results are shown in Table 2. The recovery rates of the CLB in beef are all between 90% and 110%, which shows that the method can be used in the real samples with effective and acceptable results.

Table 2. Determination of CLB in bovine meat sample using Pt-LIG.

Sample	Added (μM)	Found (μM)	Recovery (%)
Beef	0	–	–
	1.00	0.97	97.00
	5.00	4.69	93.80

4. CONCLUSIONS

This work prepared a 3D porous LIG electrode on a polyimide PI film in one step by laser direct writing technology, and the LIG electrode was modified with Pt nanoparticles by chemically reduced with sodium borohydride and chloroplatinic acid. Compared with LIG electrode, Pt-LIG electrode has higher conductivity, larger surface area and better electrocatalytic ability. It is used as a new type of electrochemical sensing platform for electrochemical detection of CLB with a wide linear range of 0.1 – 820.9 μM, sensitivity of 0.2383 μA μM^{-1}, and a lower LOD of 0.072 μM. Which also exhibits enzyme-like characteristics, and its value of K_m and I_{max} was 96.77 μM and 4.82 μA, respectively. In addition, CLB was detected in the real sample of beef, and the effective and acceptable recovery rate was obtained. This work has successfully developed a fast, simple, and sensitive detection method to analyze CLB residues in meat products, providing a promising alternative method for CLB conventional sensing applications.

ACKNOWLEDGMENTS
The work was supported by the National Natural Science Foundation of China (32060760), China Agriculture Research System of MOF and MARA (CARS-37), Development and Nutrition of Feed for Beef Cattle in Guang Chang County (09005392), National College Student Innovation and Entrepreneurship Training Project of China (202110410010).

References

1. E. D. Minot, A. M. Janssens, I. Heller, H. A. Heering, C. Dekker and S. G. Lemay, *Appl. Phys. Lett.*, 91 (2007) 093507.
2. J. Yin, J. Kim, H. U. Lee and J. Y. Park, *Thin Solid Films*, 660 (2018) 564-571
3. P. Blake, E. W. Hill, A. H. Castro Neto, K. S. Novoselov, D. Jiang, R. Yang, T. J. Booth and A. K. Geim, *Appl. Phys. Lett*., 91 (2007) 063124
4. K. I. Bolotin, K. J. Sikes, Z. Jiang, M. Klima, G. Fudenberg, J. e. Hone, P. Kim and H. L. Stormer, *Solid State Commun*., 146 (2008) 351-355
5. B. Liu and K. Zhou, *Progress in Materials Science*, 100 (2019) 99-169
6. K. S. Novoselov, A. K. Geim, S. V. Morozov, D. Jiang, Y. Zhang, S. V. Dubonos, I. V. Grigorieva and A. A. Firsov, *Science*, 306 (2004) 666-669
7. S. Park and R. S. Ruoff, *Nat. Nanotechnol*., 4 (2009) 217-224
8. L. Gao, G. X. Ni, Y. Liu, B. Liu, A. H. C. Neto and K. P. Loh, *Nature*, 505 (2014) 190-194
9. W. S. Hummers Jr and R. E. Offeman, *J. Am. Chem. Soc*., 80 (1958) 1339-1339
10. Y. Zhu, S. Murali, W. Cai, X. Li, J. W. Suk, J. R. Potts and R. S. Ruoff, *Adv. Mater*., 22 (2010) 3906-3924.
11. J. Lin, Z. Peng, Y. Liu, F. Ruiz-Zepeda, R. Ye, E. L. Samuel, M. J. Yacaman, B. I. Yakobson and J. M. Tour, *Nat. Commun*., 5 (2014) 5714.
12. R. Ye, D. K. James and J. M. Tour, *Acc. Chem. Res*., 51 (2018) 1609-1620.
13. L. X. Duy, Z. Peng, Y. Li, J. Zhang, Y. Ji and J. M. Tour, *Carbon*, 126 (2018) 472-479.
14. E. Stolyarova, K. T. Rim, S. Ryu, J. Maultzsch, P. Kim, L. E. Brus, T. F. Heinz, M. S. Hybertsen and G. W. Flynn, *Proceedings of the National Academy of Science*s, 104 (2007) 9209-9212
15. R. Dreyfus, *Appl. Phys*. A, 55 (1992) 335-339.
16. Y. Zhu, P. Liu, T. Xue, J. Xu, D. Qiu, Y. Sheng, W. Li, X. Lu, Y. Ge and Y. Wen, *Microchem. J.*,

162 (2021)
17. Z. Chen, W. Ren, L. Gao, B. Liu, S. Pei and H. M. Cheng, *Nat. Mater.*, 10 (2011) 424-428.
18. X. Xuan, H. S. Yoon and J. Y. Park, *Biosens. Bioelectron.*, 109 (2018) 75-82
19. W. Li, B. Chen, H. Zhang, Y. Sun, J. Wang, J. Zhang and Y. Fu, *Biosens Bioelectron*, 66 (2015) 251-258.
20. J. Liu, L. Meng, Z. Fei, P. J. Dyson and L. Zhang, *Biosens Bioelectron*, 121 (2018) 159-165.
21. L. Wang, M. Xu, Y. Xie, Y. Song and L. Wang, *J. Mater. Sci.*, 53 (2018) 10946-10954.
22. A. A. Al-Majed, N. Y. Khalil, I. Khbrani and H. A. Abdel-Aziz, in Profiles of Drug Substances, Excipients and Related Methodology, *Elsevier*, 2017, vol. 42, pp. 91-123.
23. R. Ji, S. Chen, W. Xu, Z. Qin, J. F. Qiu and C. R. Li, *Microchimica Acta*, 185 (2018) 1-10.
24. Y. Ge, P. Liu, L. Xu, M. Qu, W. Hao, H. Liang, Y. Sheng, Y. Zhu and Y. Wen, *Food Chem.*, 371 (2022) 131140.
25. N. Duan, S. Qi, Y. Guo, W. Xu, S. Wu and Z. Wang, *LWT*, 134 (2020) 110017.
26. Y. Ge, M. B. Camarada, L. Xu, M. Qu, H. Liang, E. Zhao, M. Li and Y. Wen, *Microchimica Acta*, 185 (2018) 1-10.
27. X. Zhu, L. Lin, R. Wu, Y. Zhu, Y. Sheng, P. Nie, P. Liu, L. Xu and Y. Wen, *Biosens. Bioelectron.*, 179 (2021) 113062.
28. Y. Zhu, P. Liu, T. Xue, J. Xu, D. Qiu, Y. Sheng, W. Li, X. Lu, Y. Ge and Y. Wen, *Microchem. J.*, 162 (2021) 105855
29. M. Li, P. Zhou, X. Wang, Y. Wen, L. Xu, J. Hu, Z. Huang and M. Li, *Comput. Electron. Agric.*, 191 (2021)
30. X. Yang, B. Feng, P. Yang, Y. Ding, Y. Chen and J. Fei, *Food Chem.*, 145 (2014) 619-624.
31. L. Wang, R. Yang, J. Chen, J. Li, L. Qu and P. d. B. Harrington, *Food Chem.*, 164 (2014) 113-118.
32. C. Zhao, G. P. Jin, L. L. Chen, Y. Li and B. Yu, *Food Chem.*, 129 (2011) 595-600.
33. C. Wu, D. Sun, Q. Li and K. Wu, *Sens. Actuators*, B, 168 (2012) 178-184.
34. Y. Ge, M. Qu, L. Xu, X. Wang, J. Xin, X. Liao, M. Li, M. Li and Y. Wen, *Mikrochim. Acta*, 186 (2019) 836.
35. T. Jacobsen and K. West, *Electrochim. Acta*, 40 (1995) 255-262.
36. E. Laviron, *J. Electroanal. Chem. Interfacial Electrochem.*, 101 (1979) 19-28.
37. X. Zhu, P. Liu, Y. Ge, R. Wu, T. Xue, Y. Sheng, S. Ai, K. Tang and Y. Wen, *J. Electroanal. Chem.*, 862 (2020)
38. Y. Wen, J. Xu, M. Liu, D. Li, L. Lu, R. Yue and H. He, *J. Electroanal. Chem.*, 674 (2012) 71-82